Clays and Clay Minerals, Vol. 46, No. 1, 1–9, 1998.

KAOLIN MINERALOGY OF CLAYS IN PALEOSOL PROFILES ON THE LATE-MIOCENE SEDIMENTS IN PENGHU ISLANDS (PESCADORES), TAIWAN

WEI-MIN WANG,[1] HSUEH-WEN YEH,[2] PEI-YUAN CHEN[3] AND MING-KUANG WANG[1]

[1] Soil Laboratory, Graduate Institute of Agricultural Chemistry, National Taiwan University, Taipei, Taiwan, Republic of China

[2] Institute of Earth Sciences, Academia Sinica, Nankang, Taipei, Taiwan, Republic of China

[3] Department of Earth Sciences, National Taiwan Normal University, Taipei, Taiwan, Republic of China

Abstract—Clay mineral compositions from 2 paleosol profiles (Chu-Wan, CW, and Shiao-Men Yu, SMY, profiles) on the late-Miocene sediments in Penghu Islands (Pescadores), Taiwan, are characterized by random X-ray powder diffraction (XRD) and transmission electron microscopy (TEM). By the clay assemblage of the paleosol profile, we want to explore the probable formation mode of the Penghu paleosols.

The paleosol profiles in study are overlain by a layer of basalt flow. However, the clay mineralogy of the 2 paleosols was not altered metasomatically after burial. Results show that 3 distinctive zones of different dominating kaolin-group minerals are apparent in the profiles. In descending order, they are: 1) spheroidal, hollow 7Å-halloysite, 2) platy, irregular-shaped and disordered kaolinite, and 3) platy, irregular-shaped, disordered kaolinite. The relative crystallinity of kaolin minerals of the 3 layers is: layer 2 > layer 3 > layer 1. On the basis of the XRD, TEM analyses and the crystallinity calculations, the distribution of kaolin in Penghu paleosol profiles appears to be unique. Penghu paleosol profiles show systematic change in kaolin crystallinity and polymorphs with depth. Because the clay type is heterogeneous within the profile, this represents that Penghu paleosol profiles were polypedogenic.

The contact between the upper basalt and the paleosol is the erosion surface, so we do not know exactly what the thickness of the original paleosol was. The first layer (about 20 cm) of the profiles appears to be constituents of the original paleosol. It contains high contents of pedogenic (*in situ* weathering) hematites and 7Å-halloysites, which implies that the local climate of the Penghu Islands at late Miocene was warm and humid. Intense leaching and dry/wet cycle should be the reason for high contents of halloysite (>60%) in the Penghu paleosols. Laterization was the probable pedogenic process for the formation of the paleosols.

Key Words—7Å-Halloysite, Kaolinite, Late Miocene, Laterization, Paleosol.

INTRODUCTION

Research about clay minerals in paleosols is well documented in the literature. Several investigators utilized clay minerals in paleosols or weathered zones to reconstruct the paleoclimate (Singer 1979/1980; Bird and Chivas 1989; Giral et al. 1993; Stern et al. 1996). Paleosol is the whole or part of the soil profile that represents a former land surface. It could preserve the climatic information of the past if it was not greatly altered during and after burial (Holland and Zbinden 1988; Retallack 1988).

Chen (1992) began to investigate the field localities of some paleosols in Penghu Islands (Pescadores), Taiwan, and explained the geology and stratigraphy of these paleosols. Wang et al. (1996) studied some reddish, paleosol profiles on sediments of this area and built up the field morphological database on them, such as the paleosol structure and paleosol horizonation. According to their studies, some red paleosols contain large amounts of kaolin minerals and pedogenic hematite-nodules. These characteristics imply that these paleosols had experienced a climate that favored hydrolysis in the past (van Houten 1961; Jenny 1980). However, the detailed kaolin mineralogy is still unknown. The minor structural information among the kaolin-group minerals, such as the crystallinity of the structure and the variation of particle morphology, could reflect different crystallization condition in profiles.

The existence of kaolin mineral in soil profiles could reflect the climatic condition when the soil formed. Kaolin usually dominates in the weathered zone of tropical or subtropical areas. The most common kaolin polymorphs that occur in soils are kaolinite and halloysite. The accurate identification of the 2 minerals, especially when mixed with other 2:1 type clay minerals, is often difficult in soil research, partly because of interference by soil organic matter and iron-oxide coatings, or the overlap of the XRD basal reflection (001) of halloysite or kaolinite with that of the second order of 2:1 type clay minerals. The latter is usually the main reason for the wrong identification of the kaolin minerals. The oriented XRD specimen is usually applied to the soil

Copyright © 1998, The Clay Minerals Society

https://doi.org/10.1346/CCMN.1998.0460101 Published online by Cambridge University Press

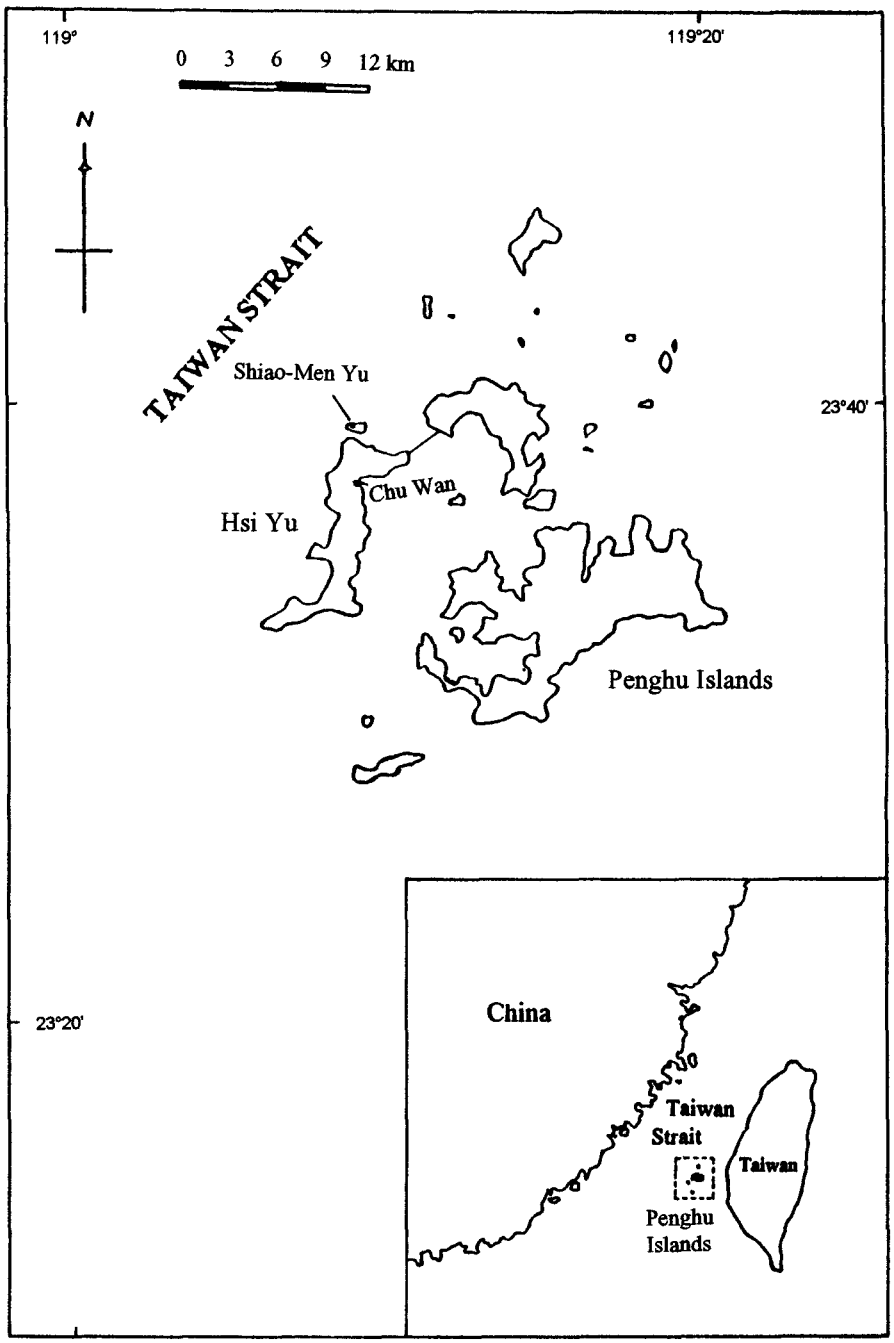

Figure 1. The locations of the Penghu Islands, Taiwan. The sampling localities and the Chu-Wan (CW) and Shiao-Men Yu (SMY) paleosol profiles are shown.

clay characterization. It enhances the *z*-axis orientation (basal reflection), but the information of the *xy* plane in structure from XRD pattern of the kaolin mineral will be missed by oriented XRD investigation. Penghu paleosols contain the single clay assemblage. They provide an optimum material to investigate the mineralogy of kaolin minerals by random powder XRD analysis and TEM observation.

This paper documents the detailed identification of kaolin minerals in the paleosol profiles on the late-Miocene sediments of the Penghu Islands, Taiwan. From the standpoint of pedogenesis, the objective is

https://doi.org/10.1346/CCMN.1998.0460101 Published online by Cambridge University Press

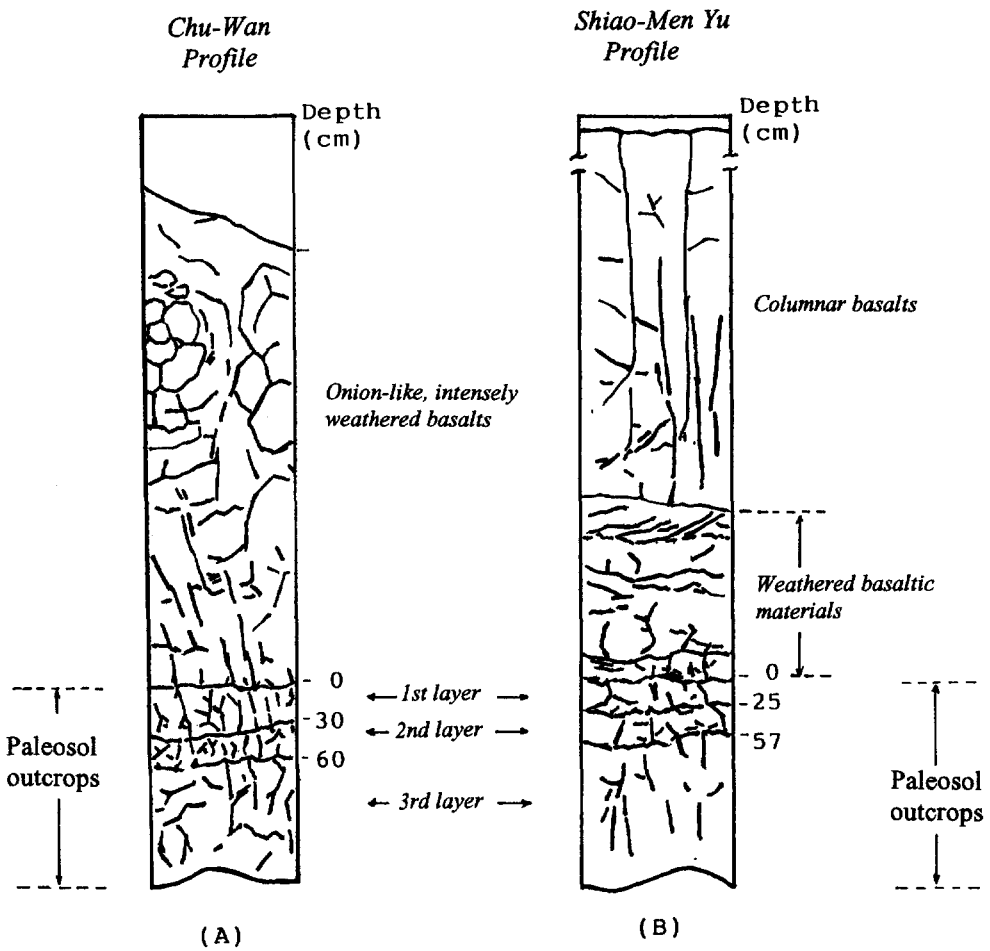

Figure 2. The geologic setting of the CW (A) and SMY (B) paleosol profiles. The paleosol outcrops are underlying the layer of basalt lava.

to explore the probable mode of formation of the kaolin minerals in the paleosols.

MATERIALS AND METHODS

Geological Background

The Penghu Islands (Pescadores) are located offshore to the west of Taiwan (Figure 1). They are covered with layers of basalt lava interbedded with several layers of muddy clastic sediments. Several localities of paleosol outcrops are observed in the Islands. These paleosols underlie a layer of basalt lava of 5 to 20 m in thickness, and are situated at the disconformity between the upper basalts and the lower sediments. The topmost 20–60 cm of the profiles were characterized as paleosols that were based on the pedogenic features of clay-rich layer, blocky to angular blocky soil structures with argillans and some fossil rootlets (Wang et al. 1996). According to the eustatic curves (Haq et al. 1987; Crowley and North 1991), global relative sea level decreased at 10–11 Ma. In addition, during the late Miocene, there was a long intervolcanic period in Penghu Islands (Chen 1992; Lee 1994). Owing to the long exposure of sediments and the climatic effect on sediments at 10 Ma, the soil developed. Therefore, it is believed that these paleosols were formed at 10 Ma, and probably exposed to the atmosphere for at least 1 million y (Chen 1992; Lee 1994). Nevertheless, the information about the parent materials is required. Because the parent materials were almost weathered, they must be reconstructed from the mineralogical composition in profiles. Results show that the parent materials of some paleosol profiles were sediments, not basaltic materials.

Two late-Miocene paleosol profiles in Penghu Islands, CW and SMY profiles, were selected for this study. Their parent materials were characterized as sediments by mineralogical investigation, but we could not observe the parent rock in the field. The general locations of the 2 sites are shown in Figure 1, and the geologic setting of the 2 profiles is shown schemati-

https://doi.org/10.1346/CCMN.1998.0460101 Published online by Cambridge University Press

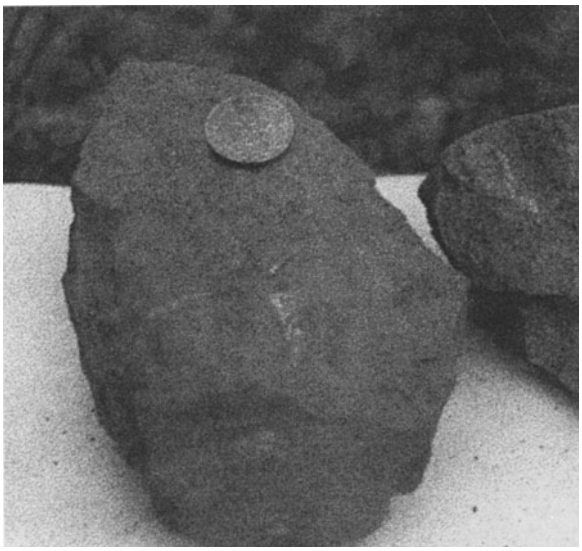

Figure 3. The fossil rootlets in Chu-Wan paleosol (Wang et al. 1996).

cally in Figure 2. The CW paleosol profile is overlain by 1 layer, 5 to 7 m in thickness, of onion-like, intensely weathered basalt (Figure 2A). The SMY paleosol profile is covered by 1 layer of columnar basalt and another layer of weathered basaltic materials, as shown in Figure 2B. Both of the 2 paleosol profiles are conspicuously reddish in color (Munsell soil color 10R). The 2 paleosol outcrops are about 2 m thick (Figure 2).

Three distinctive zones (layers) appear in each profile. The clay (<2 μm) contents of the 3 layers, in descending order, of the 2 outcrop samples are about 60, 80 and 70% (w/w). Their amounts of free iron oxides (CBD method) are 9.8, 6.9 and 6.8%. This represents that the paleosol profiles are rich in clays and iron oxides. The contact between the top of the paleosol and the overlying basalt is an erosion surface, so we do not exactly know what the thickness of the original paleosols before burial was. In layer 1, few fossil rootlets are found. They extend downward and are branched (Figure 3), and are filled with 1:1 type clays and iron hydroxyoxides (Wang et al. 1996). The fossil rootlet is a reliable item of evidence to identify a paleosol in the field (Retallack 1988). Associated with other pedogenic features, such as soil structure and soil horizonation, layer 1 is the topmost paleosol in profiles. Layer 2, compared to layer 1 and layer 3, is a hard, dark-reddish-colored (Munsell color 10R 4/8), tightly compacted layer. It also appears to have pedogenic features, but no fossil root traces are observed. The bulk density of layer 2 is higher than that of layers 1 and 3. Layer 3 is morphologically similar to layer 1, and is thicker than the upper 2 layers. The boundary between layer 1 and 2 or layer 2 and 3 is sharp and clear. From the field morphology, the paleosol profiles were polypedogenic.

Analytical Techniques

The clay mineralogy in the 3 layers of the CW and SMY paleosol profiles was characterized by 2 methods: 1) random XRD, and 2) TEM analysis.

Clay fraction (<2 μm) in samples was purified by chemical treatments. Carbonates, organic matter and free iron oxides were removed by 0.001 *M* HCl, 30% H_2O_2 and the Citrate–Bicarbonate–Dithionite (CBD) method (Kunze and Dixon 1986), respectively. Clay particles were separated after settling under gravity according to Stokes' Law (Jackson 1969). Separated clays were centrifugated, washed 3 times with deionized water (40 mL/time), freeze-dried and saved in glass bottles.

X-ray powder diffractograms were made with a Rigaku Miniflex diffractometer using Ni-filtered Cu*K*α radiation and step scanning in steps of 0.02 °2θ at a rate of 2 °2θ/min. Georgia kaolin (KGa-1), which was supplied by the Clay Minerals Society, was also pretreated the same as paleosol samples and was used to check the precision. The basal reflections of KGa-1 are 7.216 ± 0.006 Å (001), 3.592 ± 0.004 Å (002) and 2.392 ± 0.005 Å (003). Preferentially oriented specimens were employed to check for the presence of non-kaolin minerals. The XRD pattern of randomly oriented specimen could provide some useful information about 7Å-kaolin minerals.

An HITACHI H-7100 TEM was also utilized to differentiate halloysite from kaolinite according to the particle morphology. Before mounting for TEM and after chemical pretreatments the clays were ultrasonically dispersed. The clay suspension (clay:deionized water = 50 mg:400 mL) in the beaker was ultrasonicated for 15 min. One drop of suspension was added to a carbon-coated grid, which was stored in a desiccator under vacuum for 1 d. The operating voltage for TEM analysis was 75 kV.

RESULTS AND DISCUSSION

Kaolin Minerals in Clay Fractions of the Paleosol Profiles—XRD and TEM

A previous report indicated that the CW and SMY paleosol profiles in Penghu Islands contained large amounts of 7Å-kaolin minerals, but the characterization was based on the oriented XRD specimen (Wang et al. 1996). It is necessary to check the detailed mineralogy of 7Å-kaolin mineral for our purpose. The randomly mounted X-ray powder diffractogram of kaolin minerals is one of the methods to differentiate 7Å-halloysite from kaolinite (Brindley 1980). Figure 4 illustrates the randomly oriented XRD patterns of clays in each layer of the CW and SMY paleosol profiles. The relative intensity (counts per second, cps) and *d*-

https://doi.org/10.1346/CCMN.1998.0460101 Published online by Cambridge University Press

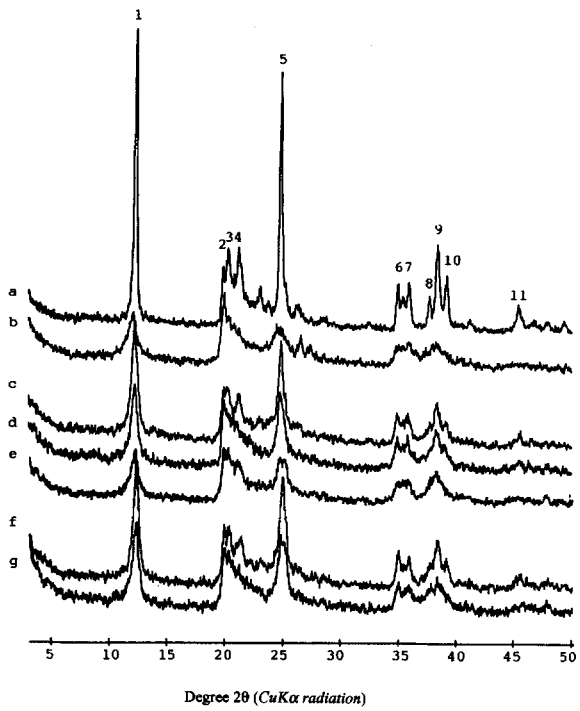

Figure 4. The randomly oriented XRD patterns of clay fractions in 3 layers of the CW and SMY paleosol profiles. a) Georgia kaolin, KGa-1; b, c, d) the first, second and third layers of the CW profiles; e, f, g) the first, second and third layers of the SMY profiles. The XRD peak numbers, 1–11, and the *d*-spacing and relative intensities (cps) are listed in Table 1.

spacing of XRD peaks of clay samples observed on Figure 4 are listed in Table 1. The XRD results indicated that the clay mineral in layer 1 of the CW and SMY profiles was 7Å-halloysite (Figures 4b and 4e). The identification of 7Å-halloysite followed the method of Brindley (1980).

The 001 and 002 diffraction peaks of clay mineral in layer 1 of the 2 profiles are 7.33 and 3.63 Å, respectively (Table 1). The intensity of the 02*l*, 11*l* diffraction bands, where the maximum is at 4.48 Å (020), is larger than the intensity of 001 and 002 basal diffraction peaks. These criteria all infer the properties of 7Å-halloysite.

Clay minerals in layer 2 of the CW and SMY profiles were characterized as disordered kaolinites (Figures 4c and 4f). The order/disorder of kaolin minerals in this study was compared to the highly crystalline kaolin, KGa-1. The 001 peak of the KGa-1 is much sharper than the 001 peak of the paleosol samples (Figure 4a). Compared to 7Å-halloysite in layer 1, the XRD patterns of the disordered kaolinites in layer 2 include triplet diffraction peaks (4.48, 4.39 and 4.20 Å) at the range of 18–22 °2θ and 2 doublet diffractions (2.57 and 2.50; 2.34 and 2.30 Å) at the range of 34–40 °2θ. Clay minerals in layer 3 of the 2 profiles are also characterized as disordered kaolinites. Their XRD patterns (Figures 4d and 4g) show the broadly spreading peaks at the range of 18–22 °2θ; however, the intensity of 001 (7.26 Å) and 002 (3.60 Å) basal reflections, unlike 7Å-halloysite in layer 1, is larger than that of the 02*l*, 11*l* diffraction bands. The *d*-spacing of the 001 and 002 peaks of 7Å-halloysite is about 0.05 Å larger than that of kaolinite. This could result from the water molecules in the structure of halloysite. Thus, the XRD characterization indicated a mineral sequence of the 3 layers as 7Å-halloysite, disordered kaolinite and disordered kaolinite.

Figure 5 demonstrates the clay morphology by TEM investigation in the 3 layers of the CW and SMY paleosol samples. KGa-1 was also observed as the reference clay. It showed hexagonal and platy kaolinite (Figure 5a). Clays in layer 1 of the CW profile consist mainly of hollow and spheroidal particles (0.15–0.25 μm in diameter), which are characterized as halloysites (Figures 5b and 5c), but clays in layer 2 are mainly irregular, hexagonal-like, platy kaolinites (Figure 5d). The third layer also contains many irregular, hexagonal-like, platy kaolinites (0.1–0.2 μm in diameter,

Table 1. The *d*-spacing (Å), and counts per second (cps) of the XRD peaks of samples from Figure 4.

Sample no.†		a		b		c		d		e		f		g	
Sample name		KGa-1		CW-1st		CW-2nd		CW-3rd		SMY-1st		SMY-2nd		SMY-3rd	
Peak no.	*hkl*	*d*-spacing	cps	*d*-spacing	cps	*d*-spacing	cps	*d*-spacing	cps	*d*-spacing	cps	*d*-spacing	cps	*d*-spacing	cps
1	001	7.21	529	7.33	139	7.26	242	7.25	172	7.30	143	7.27	267	7.22	191
2	020	4.48	122	4.47	183	4.47	125	4.48	148	4.49	148	4.48	144	4.47	148
3	110	4.39	154			4.41	126					4.38	140		
4	111	4.20	156			4.20	115					4.18	123		
5	002	3.59	455	3.64	119	3.59	209	3.60	161	3.62	129	3.58	231	3.60	170
6	130	2.57	94	2.56	77	2.57	82	2.57	86	2.57	78	2.57	99	2.57	90
7	131	2.50	96	2.50	84	2.51	82	2.51	92	2.51	83	2.50	89	2.50	85
8	003	2.39	74	2.41	74	2.39	67	2.42	59	2.39	84	2.40	70	2.38	88
9	202	2.35	161	2.34	82	2.35	103	2.35	101	2.35	101	2.35	118	2.35	100
10	131	2.30	109			2.30	67	2.31	76			2.31	86	2.32	81
11	203	2.00	61	2.00	44	1.99	54	2.00	51	2.01	45	2.00	56	1.98	56

† The sample number follows Figure 4.

https://doi.org/10.1346/CCMN.1998.0460101 Published online by Cambridge University Press

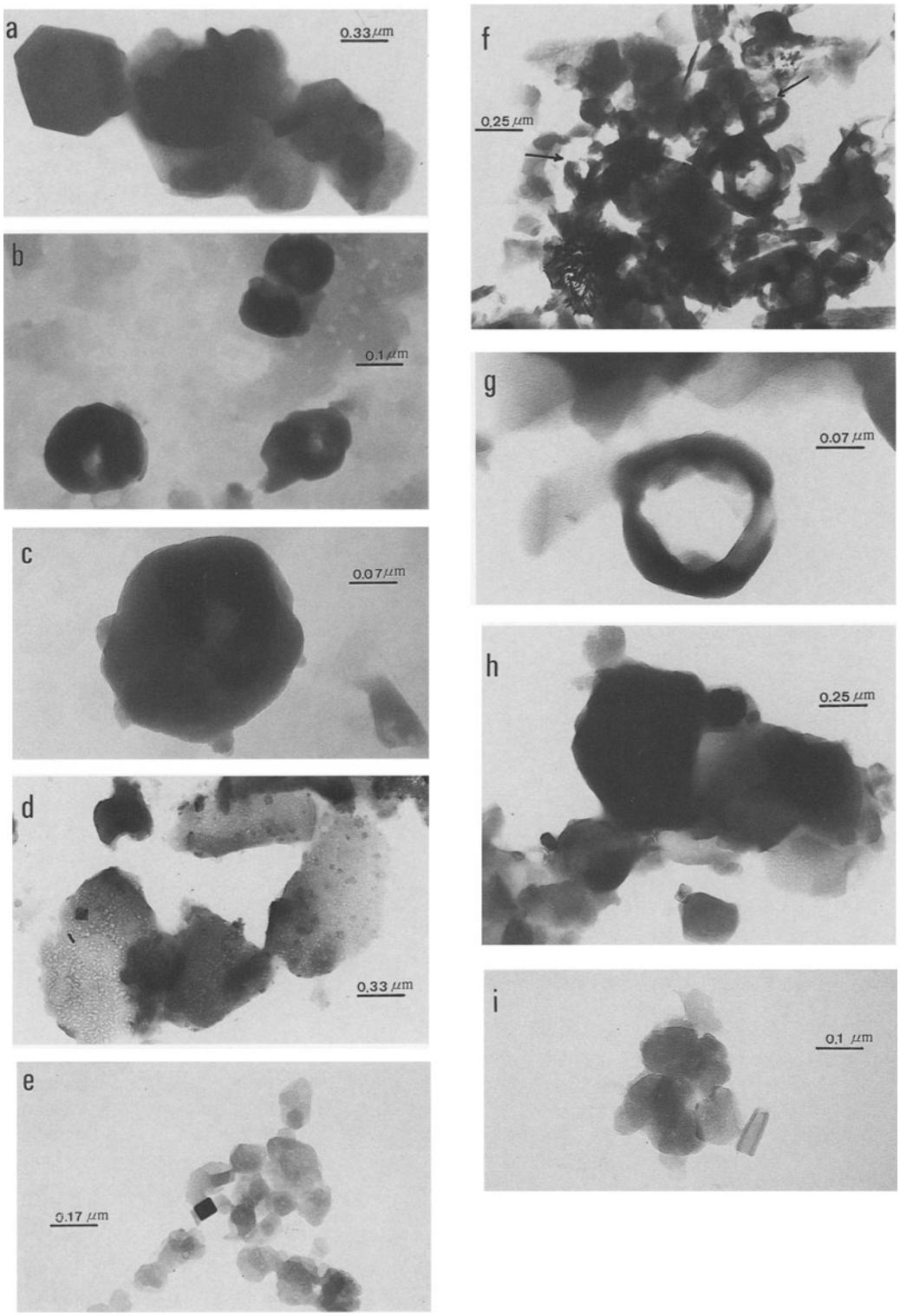

Figure 5. The TEM images of the clay fractions of the CW and SMY paleosol profiles. a) Georgia kaolin, KGa-1; b, c) clays of the first layer of the CW profile, which indicate the 0.15–0.25 μm in diameter of hollow, spheroidal halloysite; d) sub-hexagonal, platy and corroded particles of kaolinite in the second layer of the CW profile; e) some platy, corroded and sub-hexagonal kaolinites in the third layer of the CW profile; f, g) hollow, spheroidal halloysite particles in the first layer of the SMY profile; h, i) clay particles of the second and third layers of the SMY profile, indicates corroded, sub-hexagonal, and platy kaolinite particles.

https://doi.org/10.1346/CCMN.1998.0460101 Published online by Cambridge University Press

Table 2. The crystallinity of the kaolins in paleosol-like columns of the Penghu Islands.

Sample	Relative crystallinity†	C.I. of kaolinite‡
KGa-1	79.5	1.11
Chu-Wan profile (CW)		
1st layer	10.3	—
2nd layer	35	0.67
3rd layer	21.8	—
Shiao-Men Yu profile (SMY)		
1st layer	10.2	—
2nd layer	29	0.76
3rd layer	15.8	—

† Relative crystallinity = (001 peak height) ÷ (width at ½ peak height).

‡ C.I. of kaolinite is based on Hinckley's method (Hinckley 1963).

Figure 5e). The SMY profile contains spheroidal, hollow, ring-like halloysite in the first layer (Figures 5f and 5g). The SMY halloysite is 0.1–0.25 μm in diameter, similar to the CW halloysite. Some broken rings of halloysite particles are observed (the arrow in Figure 5f). Particles in the other 2 layers have the same morphology as particles in the CW profile (Figures 5h and 5i).

The morphology of halloysite in the CW and SMY samples differs slightly. The particle size (0.1–0.25 μm) is similar to the reports of Dixon and McKee (1974). There is a narrow and small hole in the center of the CW halloysite; however, the SMY halloysite has a large hollow, 0.2 μm in diameter, which is rolled from flat platy sheets. The corroded, irregular shape of kaolinite particles in the second and third layers might be caused by their poor crystallinity, so that the particle was easily destroyed by the previous chemical treatments. In addition, the electron beam of TEM could destroy the particle and cause the surface of particles to be decomposed and bubbled (Figures 5d and 5h). The kaolinite particles of the paleosol profiles are smaller than the KGa-1 kaolinite. All these properties infer that the kaolinite in Penghu paleosol profiles is disordered and poorly crystalline.

Combined with the results of the randomly oriented XRD analysis and TEM observation, the 7Å-halloysite and kaolinite could be distinguished. Briefly, the descending distribution of clay minerals of the 3 layers of the CW and SMY paleosol-like columns is: spheroidal, hollow 7Å-halloysite; platy, irregular, hexagonal-like, disordered kaolinite; and platy, irregular, hexagonal-like, disordered kaolinite.

The Crystallinity of Kaolin Minerals in the Clay Fraction

Results from XRD and TEM analyses do not clearly point out the variation of clays in layer 2 and layer 3. This could be overcome by crystallinity calculation. The relative crystallinity of all of the 3 different kaolin minerals and KGa-1 was evaluated by the intensity of the 7-Å (001) peak (peak height ÷ width at ½ peak height). Table 2 illustrates the calculated crystallinity of samples. Besides this, the crystallinity index (C.I.) of the poorly crystalline kaolinite in layer 2 of the CW and SMY profiles was calculated by Hinckley's method (Hinckley 1963). Owing to the 02*l*, 11*l* broadly spreading bands (18–22 °2θ), the disordered kaolinite in layer 3 could not be evaluated by this method. The relative crystallinity of both the CW and SMY kaolin minerals is: layer 2 > layer 3 > layer 1 (Table 2). This result is reasonable because the crystal structure of kaolinite is more ordered than that of halloysite. The crystallinity of 7Å-halloysite of the CW samples (10.3) is slightly greater than that of the SMY samples (10.2). The 7Å-halloysite is one of the constituents of the Penghu paleosols so that the slight difference of crystallinity means that the CW and SMY halloysites were formed under similar soil environments. In addition, halloysite usually occurs under the regime of high water contents (Dixon 1989). Therefore, the 7Å-halloysite in the Penghu paleosols should be formed in adequate water condition.

The second, kaolinitic layer of the profiles is a special formation. Not only it is darker red but also it has higher bulk density compared to the upper halloysitic layer and the lower kaolinitic layer (Wang et al. 1996). The Hinckley C.I. of the CW and SMY disordered kaolinite is 0.67 and 0.76, respectively, which is between the value of poorly- and well-crystallized kaolinite (Hassanipak and Eslinger 1985). The crystallinity of KGa-1 kaolinite is 1.11 in this study, which is greater than that of the paleosol samples. The crystallinity calculations could help to clearly differentiate the difference between kaolinite in layer 2 and layer 3.

As discussed above, the kaolin mineral type among the profiles is heterogeneous, and the crystallinity of kaolinite and halloysite is different. Both profiles show systematic change in kaolin crystallinity and polymorphs with depth.

Genesis of Halloysites in Penghu Paleosol Profiles

Several models suggest that the formation modes of halloysite produce different particle shapes. As reviewed by Romero et al. (1992) and the study of Banfield and Eggleton (1990), tubular halloysite may derive from feldspar weathering as a space-filling minerals, and spheroidal halloysite may crystallize directly from the protocrystalline precursor in solution.

The clay content of the Penghu paleosol profiles is about 60%, and the clay mineralogy is spheroidal 7Å-halloysite only. Such high content of halloysite in soil profiles could be interpreted as the leaching and concentrated effect of the dry and wet cycle. Most spheroidal halloysites reported in soil profiles are formed from the Si-Al gel in soil solution (Banfield and Eggleton 1990; Ward and Roberts 1990). If leaching was

https://doi.org/10.1346/CCMN.1998.0460101 Published online by Cambridge University Press

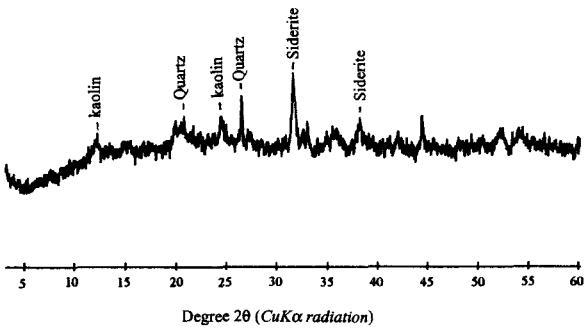

Figure 6. The X-ray diffractogram of the silt fraction of Shiao-Men Yu paleosol. Ka = Kaolin; Qz = Quartz; Sid = Siderite.

dominant during the period of soil formation, this intensely weathering process caused the decomposition of the primary minerals and 2:1 type of clay minerals. Some mobile materials, such as silicic acid and cations, would be leached out of the profiles. The remaining Si-Al gels would crystallize and concentrate as halloysites when the soil was drying.

Chen (1992) reported that the sediments in the Penghu Islands contain mainly granitic and metamorphic detrital minerals that came from the Mainland by paleoriver. Granites contain about 50% feldspar, whereas the mean in sandstones is about 10% (Fuchtbauer 1974). Therefore, we assume that the initial parent materials contained as much as 50% feldspar minerals and that almost all of the Si-Al gels in soils were derived from feldspar minerals. According to the following equation (Wollast and Chou 1988):

$$\underset{\text{plagioclase}}{2NaAlSi_3O_8} + 11H^+ + 2CO_2 \rightarrow \underset{\text{halloysite or kaolinite}}{Al_2Si_2O_5(OH)_4} + 2K^+ + 2HCO_3^- + 4H_4SiO_4 \quad [1]$$

the evaluated content of the weathering product of feldspar, halloysite, was approximately 25% (w/w). The calculated content is based on the assumption of a closed system. However, soil is an open system. By alternate dry and wet cycles, the paleosol could concentrate large amounts of halloysite. This is perhaps why the Penghu paleosols contained as much as 60% (w/w) of halloysite. Leaching and concentrated model could reasonably explain the high contents of halloysite in the Penghu paleosols. The halloysites in the Penghu paleosols were the pedogenic (e.g., *in situ* weathering) products during the soil formation.

Pedogenesis of the Penghu Paleosols and the Implication of Paleoclimate at 10 Ma

The parent materials of CW and SMY paleosols were deduced by the mineralogical suite in profiles. The paleosol profiles consisted of mainly kaolin and hematite (secondary minerals) and feldspar, rutile and quartz (primary minerals) in trace amounts (Wang et al. 1996). Quartz is not the constituent of basaltic material, so it was the detrital mineral that transported it from the source and preserved it in profiles. In addition, the Penghu paleosols also contain siderite ($FeCO_3$, Figure 6) which is usually used as an indicator of depositional environment (Mozley and Wersin 1992). Therefore, the parent materials of the Penghu paleosol were of sedimentary origins.

The clay suite of weathered profiles can be utilized as a tool to reflect the climate of soil formation (Singer 1979/1980; Curtis 1990). From the standpoint of pedogenesis, because the Penghu paleosols contain large amounts of 7Å-halloysite and hematite, laterization was the major pedogenic process during the late Miocene. For the formation of halloysite, a high water content regime is favored. Thus, the local climate during the late Miocene should be warmer and humid, compared to the present dry and hot climate in the Penghu Islands.

Regarding the second and third layers of paleosol profiles, they also appear to have some pedogenic properties. However, the mineral distribution in the 3 layers is discontinuous and changes abruptly. Maybe they were former soil pedons before the halloysitic layer formed. This means that the 3 layers are different stages of formations. That is, the paleosol profiles were polypedogenic.

By 10 Ma, warming in the tropical region could be supported by the research of the paleoclimatology (Woodruff et al. 1981; Haq 1982; Crowley and North 1991). Taking account of the paleosol morphology and clay mineral types, we recommend that the local climate in the Penghu Islands at the late Miocene was warm and humid, which favored laterization.

CONCLUSIONS

Clays (<2 μm) dominate in the 2 paleosol profiles on late-Miocene sediments in the Penghu Islands, Taiwan, and kaolin minerals are the only species in the clay fraction. The clay mineralogy of the 2 paleosols was not altered metasomatically after burial. This could be proven by the evidence of the absence of illite in profiles (no potassium-metasomatism occurred). The 7Å-kaolin minerals in samples were clearly identified by random powder XRD, crystallinity calculations and the TEM analyses. From the results, the kaolin type in the 3 layers of the CW and SMY paleosol profiles is heterogeneous and is changed systematically as a function of depths. In descending order, they are 1) spheroidal and hollow 7Å-halloysite, 2) platy, irregular-shaped, disordered kaolinite and 3) platy, irregular-shaped, disordered kaolinite. The relative crystallinity of kaolin minerals in the 3 layers is: layer 2 > layer 3 > layer 1. This

https://doi.org/10.1346/CCMN.1998.0460101 Published online by Cambridge University Press

distribution pattern of kaolin clays appears to be unique. From mineralogical compositions and crystallinity in this unique occurrence, we propose that there were 3 different stages of formation before they were overlain by basalt flows, and that the paleosol profiles were polypedogenic.

Layer 1 of the paleosol profiles in the Penghu Islands was the relict soil at late Miocene. It contains large amounts of 7Å-halloysites and iron oxides (hematite), which were the pedogenic products under the influence of the warm and humid climate at late Miocene (10 Ma). Thus, the laterization process dominated the pedogenesis of the Penghu paleosols.

ACKNOWLEDGMENTS

This study is financially supported by the National Science Council, Republic of China, under the projects #NSC 83-0202-M-002-022 and #NSC 85-2611-M-002-007.

REFERENCES

Banfield JF, Eggleton RA. 1990. Analytical transmission electron microscope studies of plagioclase, muscovite, and K-feldspar weathering. Clays Clay Miner 38:77–89.

Bird MI, Chivas AR. 1989. Stable-isotope geochronology of the Australian regolith. Geochim Cosmochim Acta 53: 3239–3256.

Brindley GW. 1980. Order–disorder in clay mineral structures. In: Brindley GW, Brown G, editors. Crystal structures of clay minerals and their X-ray diffraction. London: Mineral Soc. p 125–195.

Chen PY. 1992. A review and discussion about the stratigraphic subdivisions and some problems concerning the structural geology of the Peng-Hu Islands. Central Geological Survey, R.O.C., Special Issue No. 6. p 9–38.

Crowley TJ, North GR. 1991. Paleoclimatology. New York: Oxford Univ Pr. p 183–211.

Curtis CD. 1990. Aspects of climatic influence on the clay mineralogy and geochemistry of soils, paleosols and clastic sedimentary rocks. J Geol Soc (London) 147:351–357.

Dixon JB. 1989. Kaolin and serpentine group minerals. In: Dixon JB, Weed SB, editors. Minerals in soil environments. Madison, WI: Soil Sci Soc Am. p 467–525.

Dixon JB, McKee TR. 1974. Internal and external morphology of tubular and spheroidal halloysite particles. Clays Clay Miner 22:127–137.

Fuchtbauer H. 1974. Sediments and sedimentary rocks 1. W. Germany: E. Schweizerbartche. p 24.

Giral S, Savin SM, Girard JP, Nahon DB. 1993. The oxygen isotope geochemistry of kaolinites from lateritic profiles: Implications for pedology and paleoclimatology. Chem Geol 107:237–240.

Haq BU. 1982. Climatic acme events in the sea and on land. In: Climate in earth history. Washington, DC: National Academy Pr. p 126–132.

Haq BU, Hardenbol J, Vail PR. 1987. Chronology of fluctuating sea levels since the Triassic. Science 235:1156–1167.

Hassanipak AA, Eslinger E. 1985. Mineralogy, crystallinity, O^{18}/O^{16}, and D/H of Georgia kaolins. Clays Clay Miner 33: 99–106.

Hinckley DN. 1963. Variability in "crystallinity" values among the kaolin deposits of the coastal plain of Georgia and South California. In: Swineford A, editor. Clays Clay Miner, Proc 11th Natl Conf; 1962; Ottawa, Ontario. New York: Pergamon Pr. p 229–235.

Holland HD, Zbinden EA. 1988. Paleosols and the evolution of the atmosphere: Part I. In: Lerman A, Meybeck M, editors. Physical and chemical weathering in geological cycles. Kluwer Academic Publ. p 61–82.

Jackson ML. 1969. Soil chemical analysis—Advanced course. Madison, WI: Univ of Wisconsin. 895 p.

Jenny H. 1980. Pedogenesis of horizons and profiles: In: Jenny H, editor. The soil resource, origin and behavior. New York: Springer-Verlag. p 175.

Kunze GW, Dixon JB. 1986. Pretreatment of mineralogical analysis: In: Klute A, editor. Methods of soil analysis. Part 1 (2nd ed). Agronomy Monographs Series No. 9. p 91–100.

Lee CY. 1994. Chronology and geochemistry of basaltic rocks from Penghu Islands and mafic dikes from east Fujian: Implications for the mantle evolution of SE China since late Mesozoic [Ph.D. thesis]. Graduate Institute of Geology, National Taiwan Univ, Taipei, Taiwan. 226 p.

Mozley PS, Wersin P. 1992. Isotopic composition of siderite as an indicator of depositional environment. Geology 20: 817–820.

Retallack GJ. 1988. The field identification of paleosols. In: Reinhardt J, Sigleo WR, editors. Paleosols and weathering through geologic time: Principles and applications. Geol Soc Am (Special Paper) 216:1–20.

Romero R, Robert M, Elsass F, Garcia C. 1992. Abundance of halloysite neoformation in soils developed from crystalline rocks. Contribution of transmission electron microscopy. Clay Miner 27:35–46.

Singer A. 1979/1980. The paleoclimatic interpretation of clay minerals in soils and weathering profiles. Earth Sci Rev 15: 303–326.

Stern LA, Chamberlain CP, Reynolds RC Jr, Johnson GD. 1996. Oxygen isotope evidence of climate change of Mountain Belts from pedogenic smectite in the Himalayan Molasse. Clay Miner Soc 33rd Annu Meet, Prog and Abstr. p 148.

van Houten FB. 1961. Climatic significance of red beds. In: Nairn AEM, editor. Descriptive paleoclimatology. New York: Interscience Publ. p 89–139.

Wang WM, Yeh HW, Wang MK, Chen PY. 1996. A study of some paleosols in Penghu Islands. J Chinese Agric Chem Soc 34:417–428.

Ward CR, Roberts FI. 1990. Occurrence of spherical halloysite in bituminous coals of the Sydney Basin, Australia. Clays Clay Miner 38:501–506.

Wollast R, Chou L. 1988. Rate control of weathering of silicate minerals at room temperature and pressure. In: Lerman A, Meybeck M, editors. Physical and chemical weathering in geochemical cycles. Kluwer Academic Publ. p 11–32.

Woodruff F, Savin SM, Douglas RG. 1981. Miocene stable isotope record: A detailed deep Pacific Ocean study and its paleoclimatic implications. Science 212:665.

(Received 4 October 1996; accepted 6 December 1996; Ms. 2819)

https://doi.org/10.1346/CCMN.1998.0460101 Published online by Cambridge University Press